



ALMA MATER STUDIORUM  
UNIVERSITÀ DI BOLOGNA

ARCHIVIO ISTITUZIONALE  
DELLA RICERCA

## Alma Mater Studiorum Università di Bologna Archivio istituzionale della ricerca

Quadrilateral Orbifold Splines

This is the final peer-reviewed author's accepted manuscript (postprint) of the following publication:

*Published Version:*

Quadrilateral Orbifold Splines / Beccari C.V.; Prautzsch H.. - STAMPA. - 49:(2022), pp. 1-18. [10.1007/978-3-030-92313-6\_1]

*Availability:*

This version is available at: <https://hdl.handle.net/11585/895242> since: 2022-11-15

*Published:*

DOI: [http://doi.org/10.1007/978-3-030-92313-6\\_1](http://doi.org/10.1007/978-3-030-92313-6_1)

*Terms of use:*

Some rights reserved. The terms and conditions for the reuse of this version of the manuscript are specified in the publishing policy. For all terms of use and more information see the publisher's website.

This item was downloaded from IRIS Università di Bologna (<https://cris.unibo.it/>).  
When citing, please refer to the published version.

(Article begins on next page)

This is an Author Accepted Manuscript version of the following chapter: Beccari, C.V., Prautzsch, H. (2022). Quadrilateral Orbifold Splines. In: Manni, C., Speleers, H. (eds) Geometric Challenges in Isogeometric Analysis. Springer INdAM Series, vol 49. Springer, Cham. [https://doi.org/10.1007/978-3-030-92313-6\\_1](https://doi.org/10.1007/978-3-030-92313-6_1)

Users may only view, print, copy, download and text- and data-mine the content, for the purposes of academic research. The content may not be (re-)published verbatim in whole or in part or used for commercial purposes. Users must ensure that the author's moral rights as well as any third parties' rights to the content or parts of the content are not compromised.

# Quadrilateral Orbifold Splines

Carolina Vittoria Beccari and Hartmut Prautzsch

**Abstract** Orbifold spline surfaces are closed free form surfaces of any topological genus. Their patches have  $C^k$  joints along common boundaries after linear rational reparametrizations, where  $k$  can be chosen arbitrarily. There are orbifold splines with rational triangular and – with certain restrictions on the patch layout – polynomial quadrilateral patches. Here, we present orbifold splines with rational quadrilateral patches without any restrictions on the patch layout. They are obtained from triangular orbifold splines by rational linear or bi-linear reparametrizations. With linear reparametrizations, we get discontinuously and otherwise continuously parametrized  $G^k$  surfaces.

## 1 Introduction

Constructing smooth free form surfaces necessarily requires so-called  $G^k$  constructions, i. e., reparametrizations that typically raise the degree of the polynomial patches of such surfaces. Thus, low-degree reparametrization functions are desirable and, if polynomials are used, their degree can be  $k + 1$ , where  $k$  is the smoothness order [15, 22]. In view of the degree estimates in [18, 21],  $k + 1$  seems to be the lowest possible degree in general. Therefore, it is intriguing that linear rational reparametrizations are sufficient if we work with rational patches parametrized over the hyperbolic plane. This then leads to rational orbifold splines introduced to Computer Aided Geometric Design and studied by [19, 2, 3]. The spline manifolds introduced in [7, 8] are re-

---

Carolina Vittoria Beccari  
Alma Mater Studiorum - Università di Bologna, P.zza di Porta S. Donato 5, 40126 Bologna, Italy,  
e-mail: carolina.beccari2@unibo.it

Hartmut Prautzsch  
Karlsruhe Institute for Technology, Am Fasanengarten 5, 76131 Karlsruhe, Germany e-mail:  
prautzsch@kit.edu

lated but are built with affine reparametrizations and therefore necessarily have one singular point.

The reparametrization functions for  $G^k$  constructions are called **transition functions** and linear rational transition functions are projective maps defined by the weighted vertices (see Definition 1) of a triangle and its image. Hence, if we wish to use such functions, it is natural to work with triangular patches as in the references above. Since we may replace any transition function by its  $k$ -th degree Taylor polynomial for the  $G^k$  constructions, it is also possible to come up with polynomial orbifold splines with linear rational transition functions. The degree, however, goes faster up with  $k$  than for rational orbifolds. All this has been derived by J. Peters and coauthors [13, 14, 23] using a purely algebraic approach as opposed to the geometric one employed by the other authors based on hyperbolic geometry.

Since the algebraic approach is quite involved, certain symmetry assumptions helped Peters to get it through with explicit formulae and sophisticated constructions. On the downside of it, this led to certain restrictions on the patch layout.

Although we could give up on Peters' symmetry assumption, a geometric look reveals that there are intrinsic restrictions on the patch layout if we want to work with either polynomial or rational quadrilateral patches and projective, i. e., linear rational transition functions [16] that only reparametrize cross boundary derivatives, but no patch boundaries.

In this paper, we show how to get around these problems by either projective transition functions that lead to reparametrizations of boundary curves and to  $C^{-1}$  joints of adjacent patch parametrizations or by bi-projective, i. e., bi-linear, rational transition functions contacting adjacent ones continuously.

The quadrilateral orbifold splines we present have no restrictions on their patch layout and share the same low degree with triangular orbifold splines. However, here it is a bi-degree  $n$ , whereas for triangles it is a total degree  $n$ . Furthermore, triangular orbifold  $G^k$  splines can be built with Powell-Sabin splits, or by enforcing  $G^{2k}$  supersmoothness at the vertices, or by solving simply the system of  $G^k$  conditions. Our quadrilateral orbifold splines are obtained from any such triangular splines where we pair triangles into quadrilaterals. For each pair, we require  $G^{2k}$  contact, but do this only at the two common vertices. Otherwise, we require  $G^k$  contact between different pairs.

Since the construction is based on triangular orbifold splines and to keep the paper self-contained, we first introduce the essentials of triangular orbifold spline constructions starting with a review of the hyperbolic plane in Section 2, two different Bézier representations for homogenous polynomials in Section 3, and simple  $G^k$  joints for rational polynomials that can be expressed by  $C^k$  joints of homogenous polynomials in Section 4. Then in Section 5, we explain orbifold splines, come to projective structures in Section 6 and finally in Sections 7 and 8 to the constructions of quadrilateral orbifold splines.

## 2 The Hyperbolic Plane

In this section, we briefly review three models of the hyperbolic plane  $\mathcal{H}^2$  that have been used to introduce and develop orbifold splines in [2, 3, 6, 8, 19, 24].

### The Hyperbolic Model

Most important for this paper is the **hyperbolic model** of the hyperbolic plane  $\mathcal{H}^2$ . In this model,  $\mathcal{H}^2$  is formed by the pairs  $(\mathbf{x}, -\mathbf{x})$  of points on the two-sheeted hyperboloid  $\mathcal{H}$  given by the equation

$$\mathcal{H} : \mathbf{x}^t Q \mathbf{x} = [x \ y \ z] \begin{bmatrix} 1 & & \\ & 1 & \\ & & -1 \end{bmatrix} \begin{bmatrix} x \\ y \\ z \end{bmatrix} = -1.$$

Note that the associated homogenous equation

$$C : \mathbf{x}^t Q \mathbf{x} = 0$$

defines the asymptotic cone  $C$  of the hyperboloid. We can simplify this model to the upper sheet  $\mathcal{U}$  of the hyperboloid by replacing the pairs  $(\mathbf{x}, -\mathbf{x})$  by the points  $\mathbf{x} \in \mathcal{U}$ , see Figure 1.

A hyperbolic plane has (hyperbolic) lines and any such line is a non-empty intersection of  $\mathcal{U}$  with any two-dimensional subspace of  $\mathbb{R}^3$ . The lines are preserved by the hyperbolic maps, which are the linear maps of  $\mathbb{R}^3$  restricted to  $\mathcal{U}$  that map

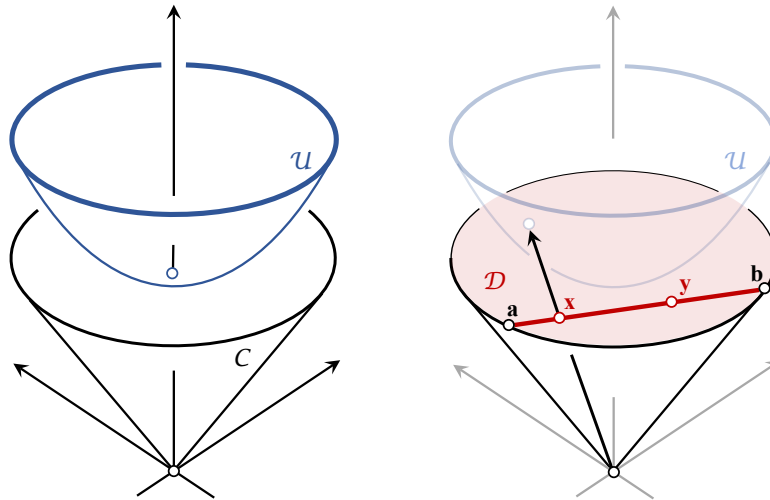


**Fig. 1** The hyperbolic (left) and the Klein model (right)  $\mathcal{H}$  of the hyperbolic plane

$\mathcal{U}$  into itself. For example, rotations around the  $z$ -axis and reflections about planes containing the  $z$ -axis represent special hyperbolic maps.

*Remark 1* If  $\mathcal{U}$  is mapped to itself by a linear map  $\mathbf{x} \mapsto A\mathbf{x}$ , then the quadratic polynomials  $\mathbf{x}^t Q \mathbf{x} - 1$  and  $(A\mathbf{x})^t Q (A\mathbf{x}) - 1$  have the same zero sets. This implies that a hyperbolic map is represented by a matrix  $A$  for which  $A^t Q A = Q$ . Such a map  $\mathbf{x} \mapsto A\mathbf{x}$  also maps the cone  $C$  onto itself. On the other hand, any linear map that maps  $C$  onto itself has a matrix  $A$  for which  $A^t Q A = Q\rho^2, \rho \neq 0$ , is a positive multiple of  $Q$  or equivalently for which any multiple  $A\rho, \rho \neq 0$ , represents a hyperbolic map.

*Remark 2* In incidence geometry, the lines form the structure of a geometry and the hyperbolic plane can be defined by Hilbert's axioms [9], [11, p. 268]. Different from that approach, Felix Klein proposed in his seminal Erlangen program (1872) to classify geometries by the invariants under an automorphism group. The hyperbolic maps form the automorphisms in hyperbolic geometry and their invariants are the lines, angles and distances.

### The Klein Model

Orbifold splines satisfy smoothness conditions based on linear rational reparametrizations. Therefore, it is natural to work with rational orbifold splines. The Klein model of the hyperbolic plane shows where the linear rational maps come from.

We obtain the Klein model by the central projection

$$\pi : \mathbb{R}^3 \setminus \{0\} \rightarrow \left\{ \begin{bmatrix} \mathbf{x} \\ 1 \end{bmatrix} \mid \mathbf{x} \in \mathbb{R}^2 \right\}, \quad \begin{bmatrix} \mathbf{x} \\ z \end{bmatrix} \mapsto \begin{bmatrix} \mathbf{x}/z \\ 1 \end{bmatrix}$$

that maps  $\mathcal{U}$  onto the open unit disk

$$\mathcal{D} : x^2 + y^2 < 1, \quad z = 1,$$

and the hyperbolic lines into straight line segments, see Figure 1. Under this projection, the linear maps in  $\mathbb{R}^3$  become the linear rational maps of the plane  $z = 1$  into itself.

*Remark 3* The set of all lines in  $\mathbb{R}^3$  through the origin forms a projective plane and we can define the lines  $[x \ y \ 0]^t \mathbb{R}$  to be its ideal points. The linear maps in  $\mathbb{R}^3$  represent the projective maps of the projective plane and projective extensions of the rational maps in the plane  $z = 1$ .

Thus, in the Klein model, the hyperbolic maps are projective maps restricted to  $\mathcal{D}$  that map the disk  $\mathcal{D}$  onto itself. Note that a projective map is represented by a linear map or a  $3 \times 3$  matrix  $A$  and that any non-zero multiple of  $A$  represents the same projective map in accordance with Remark 1.

Projective maps preserve cross ratios. This can be used to define hyperbolic distances that are invariant under hyperbolic maps: Any two hyperbolic points  $\mathbf{x}$

and  $\mathbf{y}$  span a hyperbolic line, which is the interior of a line segment  $\mathbf{ab}$  in  $\mathbb{R}^3$ . The non-hyperbolic points  $\mathbf{a}$ ,  $\mathbf{b}$  lie on the boundary of  $\mathcal{D}$  and the points on the boundary of  $\mathcal{D}$  are the **ideal points** (of  $\mathcal{H}^2$ ), see Figure 1. If we extend hyperbolic maps to the ideal points, they map them to ideal points. Thus,

$$\text{dist}(\mathbf{x}, \mathbf{y}) := \left| \log (\text{cross ratio}[\mathbf{xy}|\mathbf{ab}]) \right|,$$

is invariant under hyperbolic maps and is called the **hyperbolic distance** of  $\mathbf{x}$  and  $\mathbf{y}$ , [10, (1) on p. 214].

*Remark 4* Any three points  $\mathbf{a}, \mathbf{b}, \mathbf{c}$  on  $\mathcal{U} \subset \mathbb{R}^3$  define a hyperbolic triangle and there is a unique linear map mapping  $\mathbf{a}, \mathbf{b}, \mathbf{c} \in \mathbb{R}^3$  to the vertices in a given order of any other hyperbolic triangle. It represents a projective map in the plane  $z = 1$ . Note that it is a hyperbolic map only if it maps  $\mathcal{D}$  onto itself.

We mention this since, although the domain of an orbifold spline, which is defined in Section 5, is the hyperbolic plane, the  $G^k$  transition functions in Section 4 of an orbifold spline are such projective maps that need not be hyperbolic. Therefore, these transition functions form what is called a projective structure and we come to it in Section 6.

**Definition 1** We denote the linear span without the zero element of any vectors  $\mathbf{v}_1, \dots, \mathbf{v}_n$  by  $\langle \mathbf{v}_1, \dots, \mathbf{v}_n \rangle$  and the linear span of a matrix  $A$  without the zero matrix by  $\langle A \rangle$ . Hence, for  $n = 1$  and  $\mathbf{x} = \mathbf{v}_1$ , the preimage  $\pi^{-1}(\mathbf{x})$  is  $\langle \mathbf{x} \rangle$ . This span is the class of all (homogeneous) coordinate vectors representing the point  $\mathbf{x}$  and we also address it as the point  $\langle \mathbf{x} \rangle$ . Similarly,  $\langle A \rangle$  is the class of all (homogeneous) matrices representing the same projective map and we also call the map  $\langle A \rangle$ .

Further, we call any member  $\mathbf{v}$  of  $\langle \mathbf{v} \rangle$  a **weighted point**.

### The Poincaré Model

For illustrations, such as in Figure 4, we like to use the Poincaré model of the hyperbolic plane. It is obtained from the Klein model by mapping the disk  $\mathcal{D}$  onto itself by the map

$$\begin{bmatrix} \mathbf{x} \\ \mathbf{y} \end{bmatrix} \mapsto \begin{bmatrix} \mathbf{x} \\ \mathbf{y} \end{bmatrix} / \left( 1 + \sqrt{1 - x^2 - y^2} \right),$$

which maps the hyperbolic lines into circular arcs that meet the unit circle orthogonally. This map is a composition of the inverse of the orthogonal projection from  $\mathcal{D}$  to the lower half of the sphere with equator  $\mathcal{D}$  and the (angle and circle preserving) stereographic projection whose center is the north pole back to the disk  $\mathcal{D}$ , see Figure 2.

In the Poincaré model, the hyperbolic maps are the circle relationships that map the disk  $\mathcal{D}$  onto itself [12, Thm. 6.1 on p. 286]. Since they preserve angles, the hyperbolic maps do so too and, in this model, the **hyperbolic angles** are just the euclidean ones.

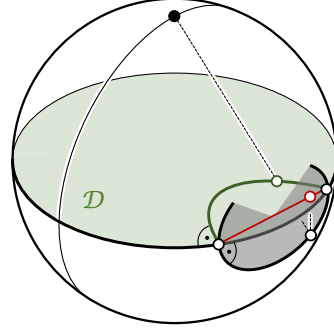


**Fig. 2** The Poincaré model (green) of the hyperbolic plane

### 3 Rational Patches and their Bézier Forms

We wish to construct piecewise rational splines mapping certain domains in the hyperbolic plane onto smooth closed surfaces. These splines consist of quadrilateral bi-rational patches obtained from pairs of triangular patches.

A triangular patch is defined over some triangle  $\mathbf{abc}$  and first we assume  $\mathbf{a}, \mathbf{b}, \mathbf{c}$  to lie in the open disk  $\mathcal{D} \subset \mathbb{R}^3$  representing the Klein model of the hyperbolic plane. With the coordinate transformation

$$\mathbf{x} = [\mathbf{a} \ \mathbf{b} \ \mathbf{c}] \mathbf{u}, \quad \mathbf{u} = \begin{bmatrix} u \\ v \\ w \end{bmatrix},$$

we write a rational polynomial of degree  $n$  as

$$\mathbf{r}(\mathbf{x}) = \frac{\mathbf{p}(\mathbf{u})}{q(\mathbf{u})}, \quad |\mathbf{u}| := u + v + w = 1,$$

or homogeneously as

$$\mathbf{r}(\mathbf{x}) = \begin{bmatrix} \mathbf{p}(\mathbf{u}) \\ q(\mathbf{u}) \end{bmatrix}.$$

With the Bernstein polynomials

$$B_{\mathbf{i}}(\mathbf{u}) = \binom{n}{\mathbf{i}} \mathbf{u}^{\mathbf{i}} := \frac{n!}{i!j!k!} u^i v^j w^k$$

for

$$\mathbf{i} = \begin{bmatrix} i \\ j \\ k \end{bmatrix} \in \Gamma_n^3 := \left\{ \mathbf{i} \in \mathbb{Z}_{n+1}^3 \mid |\mathbf{i}| = i + j + k = n \right\},$$

we get the **homogeneous Bézier form** or **homogeneous Bézier representation**



$$\mathfrak{r}(\mathbf{x}) = \sum_{\mathbf{i} \in \Gamma_n^3} \mathfrak{r}_i B_i(\mathbf{u})$$

of the rational patch.

Since any nonzero multiple of  $\mathfrak{r}$  represents the same point  $\mathbf{p}/q$ , we can omit the restriction  $|\mathbf{u}| = 1$  and extend the polynomial  $\mathfrak{r}$  to a homogeneous polynomial of degree  $n$  over  $\mathbb{R}^3$ , i. e.,

$$\mathfrak{r}(\mathbf{x}\rho) = \mathfrak{r}(\mathbf{x})\rho^n \quad \text{for any } \rho \in \mathbb{R}.$$

*Remark 5* Writing the vectors  $\mathfrak{r}_i$  as

$$\mathfrak{r}_i = \begin{bmatrix} \mathbf{r}_i \rho_i \\ \varepsilon_i \rho_i \end{bmatrix}, \quad \varepsilon_i \in \{0, 1\},$$

we see the **Bézier points**  $\mathbf{r}_i$  and **weights**  $\rho_i$ . If  $\varepsilon_i = 0$ , then  $\mathbf{r}_i$  actually is a vector on whose length the weight  $\rho_i$  depends.

*Remark 6* The homogeneous polynomial  $\mathfrak{r}(\mathbf{x})$  is completely determined by its values on any plane or surface passing through the cone

$$[\mathbf{a} \ \mathbf{b} \ \mathbf{c}] \mathbb{R}_{>0}^3.$$

In particular, we could consider  $\mathfrak{r}(\mathbf{x})$  over the hyperbolic sheet  $\mathcal{U}$  or over any triangle  $\mathbf{a}\alpha \ \mathbf{b}\beta \ \mathbf{c}\gamma$  with  $\alpha, \beta, \gamma \in \mathbb{R} \setminus \{0\}$  and derive the Bézier form of  $\mathfrak{r}$  with respect to it:

Let  $\mathbf{u}$  be the coordinate vector of any  $\mathbf{x} \in \mathbb{R}^3$  with respect to the scaled basis  $\mathbf{a}\alpha, \mathbf{b}\beta, \mathbf{c}\gamma$ , i. e.,

$$\mathbf{x} = [\mathbf{a}\alpha \ \mathbf{b}\beta \ \mathbf{c}\gamma] \mathbf{u} = [\mathbf{a} \ \mathbf{b} \ \mathbf{c}] S \mathbf{u}, \quad S = \begin{bmatrix} \alpha & & \\ & \beta & \\ & & \gamma \end{bmatrix}.$$

Then  $S\mathbf{u}$  represents  $\mathbf{x}$  with respect to the initial basis  $\mathbf{a} \ \mathbf{b} \ \mathbf{c}$  and because the Bernstein polynomials are homogeneous in each variable, we obtain from  $\mathfrak{r}$ 's Bézier form

$$\mathfrak{r}(\mathbf{x}) = \sum \mathfrak{r}_i B_i(S\mathbf{u})$$

with respect to  $\mathbf{a} \ \mathbf{b} \ \mathbf{c}$  directly the new one w.r.t.  $\mathbf{a}\alpha \ \mathbf{b}\beta \ \mathbf{c}\gamma$ :

$$\mathfrak{r}(\mathbf{x}) = \sum \mathfrak{r}_i \alpha^i \beta^j \gamma^k B_i(\mathbf{u}).$$

Note that the Bézier points  $\mathbf{r}_i$  are still the same. Only the weights  $\rho_i$  changed to  $\rho_i \alpha^i \beta^j \gamma^k$ .

*Remark 7* Substituting  $\mathbf{u}$  by  $S\mathbf{u}$  corresponds to a linear reparametrization with the map  $\mathbf{u} \mapsto S\mathbf{u}$ . If we view  $\mathfrak{r}$  as a rational polynomial  $\mathbf{r}(\mathbf{x})$  over the plane  $z = 1$ , in which  $S$  represents a projective map mapping the triangle  $\mathbf{a}\mathbf{b}\mathbf{c}$  to itself, this reparametrization is a projective reparametrization of  $\mathbf{r}(\mathbf{x})$ , see [4, p. 244].

The homogeneous polynomial  $\mathfrak{r}(\mathbf{x})$  also has an **inhomogeneous tetrahedral Bézier representation**. Since a homogeneous polynomial of degree  $n$  has zero derivatives at the origin  $\mathbf{o}$  up to degree  $n - 1$ , we easily get  $\mathfrak{r}$ 's Bézier form

$$\mathfrak{r}(\mathbf{x}) = \sum_{\mathfrak{i} \in \Gamma_n^4} \mathfrak{r}_{\mathfrak{i}} B_{\mathfrak{i}}(\mathfrak{v})$$

over the tetrahedron  $\mathbf{oabc}$  with

$$\mathbf{x} = [\mathbf{o} \ \mathbf{a} \ \mathbf{b} \ \mathbf{c}] \mathfrak{v}, \quad B_{\mathfrak{i}}(\mathfrak{v}) = \binom{n}{\mathfrak{i}} \mathfrak{v}, \quad |\mathfrak{v}| = 1,$$

and

$$\mathfrak{r}_{\mathfrak{i}} = \begin{cases} 0 & \text{for } \mathfrak{i} = \begin{bmatrix} i_0 \\ \mathbf{i} \end{bmatrix} \text{ with } i_0 > 0, \\ \mathfrak{r}_{\mathbf{i}} & \text{for } \mathfrak{i} = \begin{bmatrix} 0 \\ \mathbf{i} \end{bmatrix}. \end{cases}$$

## 4 Smooth Joints

As follows from the previous section, we can represent any piecewise rational spline over the hyperboloid  $\mathcal{U}$ , the disk  $\mathcal{D}$  or any plane  $\mathcal{E} \subset \mathbb{R}^3 \setminus \{0\}$  by a homogeneous spline  $\mathfrak{r} = \begin{bmatrix} \mathbf{p} \\ q \end{bmatrix}$ . If this spline is in  $C^k$ , then its restriction to  $\mathcal{U}$ ,  $\mathcal{D}$  or  $\mathcal{E}$  also is, and vice versa. Further, if the restriction is in  $C^k$ , then so is its central projection  $\mathbf{r} = \mathbf{p}/q$ . Although  $\mathfrak{r}$  could be less smooth than its projection, we only build rational  $C^k$  splines with  $C^k$  homogeneous representations since this is sufficient for our purpose and is the simplest.

To build such a homogeneous spline consisting of polynomial segments over pyramidal cones as  $[\mathbf{a} \ \mathbf{b} \ \mathbf{c}] \mathbb{R}^3 = \{[\mathbf{a} \ \mathbf{b} \ \mathbf{c}] \mathfrak{v} \mid \mathfrak{v} \in \mathbb{R}^3\}$ , we specify the smoothness conditions between adjacent segments using their homogeneous Bézier forms.

Given two triangles  $A = [\mathbf{a} \ \mathbf{b} \ \mathbf{c}]$  and  $B = [\mathbf{a} \ \mathbf{b} \ \mathbf{d}]$  in  $\mathbb{R}^3$  with homogeneous polynomial pieces

$$\mathfrak{r}(A\mathbf{u}) = \sum_{\mathfrak{i} \in \Gamma_n^3} \mathfrak{r}_{\mathfrak{i}} B_{\mathfrak{i}}(\mathbf{u}), \quad \mathbf{u} \geq 0,$$

and

$$\mathfrak{s}(B\mathbf{u}) = \sum_{\mathfrak{i} \in \Gamma_n^3} \mathfrak{s}_{\mathfrak{i}} B_{\mathfrak{i}}(\mathbf{u}), \quad \mathbf{u} \geq 0,$$

we use their Bézier forms

$$\sum_{\mathfrak{i} \in \Gamma_n^4} \mathfrak{r}_{\mathfrak{i}} B_{\mathfrak{i}}(\mathfrak{v}) \quad \text{and} \quad \sum_{\mathfrak{i} \in \Gamma_n^4} \mathfrak{s}_{\mathfrak{i}} B_{\mathfrak{i}}(\mathfrak{v})$$

with respect to the tetrahedra  $[\mathbf{o} \ \mathbf{a} \ \mathbf{b} \ \mathbf{c}]$  and  $[\mathbf{o} \ \mathbf{a} \ \mathbf{b} \ \mathbf{d}]$ , respectively, where

$$\mathfrak{r}_{\mathfrak{i}} = \begin{cases} \mathfrak{r}_{\mathbf{i}} & \text{if } \mathfrak{i} = \begin{bmatrix} 0 \\ \mathbf{i} \end{bmatrix} \\ \emptyset & \text{else} \end{cases}$$

and

$$\mathfrak{s}_{\mathfrak{i}} = \begin{cases} \mathfrak{s}_{\mathbf{i}} & \text{if } \mathfrak{i} = \begin{bmatrix} 0 \\ \mathbf{i} \end{bmatrix} \\ \emptyset & \text{else} \end{cases}.$$

We recall from [5] that  $\mathfrak{r}(\mathbf{x})$  and  $\mathfrak{s}(\mathbf{x})$  have equal derivatives up to order  $r$  over the plane  $\mathbf{oab}$  if and only if, for all  $k \leq r$  and all

$$\mathfrak{i} = \begin{bmatrix} i_0 \\ i \\ j \\ k \end{bmatrix} = \mathfrak{j} + \begin{bmatrix} 0 \\ 0 \\ 0 \\ k \end{bmatrix} \in \Gamma_n^4,$$

we have

$$\mathfrak{s}_{\mathfrak{i}} = \sum_{\mathfrak{k} \in \Gamma_k^4} \mathfrak{r}_{\mathfrak{j}+\mathfrak{k}} B_{\mathfrak{k}}(\mathfrak{d})$$

where

$$\begin{bmatrix} \mathbf{o} & \mathbf{a} & \mathbf{b} & \mathbf{c} \\ 1 & 1 & 1 & 1 \end{bmatrix} \mathfrak{d} = \begin{bmatrix} \mathbf{d} \\ 1 \end{bmatrix}.$$

Since most  $\mathfrak{r}_{\mathfrak{i}}$  are zero, these conditions simplify and can be written solely in terms of the  $\mathfrak{r}_{\mathbf{i}}$  and  $\mathfrak{s}_{\mathbf{i}}$ . Namely,  $\mathfrak{r}(\mathbf{x})$  and  $\mathfrak{s}(\mathbf{x})$  have  $C^r$  contact if and only if for all  $k \leq r$  and

$$\mathbf{i} = \begin{bmatrix} i \\ j \\ k \end{bmatrix} = \mathbf{j} + \begin{bmatrix} 0 \\ 0 \\ k \end{bmatrix} \in \Gamma_n^3,$$

we have

$$\mathfrak{s}_{\mathbf{i}} = \sum_{\mathbf{k} \in \Gamma_k^3} \mathfrak{r}_{\mathbf{j}+\mathbf{k}} B_{\mathbf{k}}(A^{-1}\mathbf{d}), \quad (1)$$

which has first been proved in [1], where homogeneous trivariate polynomials are used to define splines over spheres.

*Remark 8* Using the local parameters  $\mathbf{u} = A^{-1}\mathbf{x}$  and  $\mathbf{v} = B^{-1}\mathbf{x}$ , we obtain that

$$\mathfrak{p}(\mathbf{u}) := \mathfrak{r}(A\mathbf{u}) = \mathfrak{r}(\mathbf{x}) \quad \text{and} \quad \mathfrak{q}(\mathbf{v}) := \mathfrak{s}(B\mathbf{v}) = \mathfrak{s}(\mathbf{x})$$

have  $C^k$  contact after we reparametrize  $\mathfrak{p}(\mathbf{u})$  by the coordinate transformation

$$\mathbf{v} \mapsto \mathbf{u}(\mathbf{v}) = A^{-1}B\mathbf{v} = [\mathbf{e}_1 \ \mathbf{e}_2 A^{-1}\mathbf{d}]\mathbf{v}$$

taking us from system **abd** to **abc**.

Note that the matrix  $A^{-1}B$  is completely defined by the vector  $A^{-1}\mathbf{d}$  defining the  $C^r$  conditions (1). With respect to the first system **abc**, the matrix  $A^{-1}B$  represents the linear map mapping **a, b, c** to **a, b, d**, respectively.

*Remark 9* In the Klein model, the projective map  $\langle A^{-1}B \rangle$  maps the points  $\langle \mathbf{a} \rangle, \langle \mathbf{b} \rangle, \langle \mathbf{c} \rangle$  to  $\langle \mathbf{a} \rangle, \langle \mathbf{b} \rangle$  and  $\langle \mathbf{d} \rangle$ . It is determined either by the weighted points **a, b, c** and their weighted images **a, b, d** or by the (non-weighted) points  $\langle \mathbf{a} \rangle, \langle \mathbf{b} \rangle, \langle \mathbf{c} \rangle$  with the so-called unit point  $\langle \mathbf{a} + \mathbf{b} + \mathbf{c} \rangle$  and their images  $\langle \mathbf{a} \rangle, \langle \mathbf{b} \rangle, \langle \mathbf{d} \rangle, \langle \mathbf{a} + \mathbf{b} + \mathbf{d} \rangle$ . Thus, the rational polynomials  $\mathbf{r}(\mathbf{u})$  and  $\mathbf{s}(\mathbf{v})$  represented by  $\mathfrak{r}(\mathbf{u})$  and  $\mathfrak{s}(\mathbf{v})$ , respectively, have a  $C^r$  contact after a projective reparametrization. Such a contact is called a **G<sup>r</sup> contact** and the reparametrization map its **transition function**.

*Remark 10* Under a projective map  $\langle P \rangle$ , the triangles  $A$  and  $B$  are mapped to  $PA$  and  $PB$  while the matrices

$$(PA)^{-1}PB = A^{-1}B$$

of their transition functions (w.r.t. the systems  $PA$  and  $A$ , resp.) are the same.

## 5 Orbifold Splines

Any closed surface  $S$  of topological genus  $\gamma \geq 2$  can be cut open into an open surface with a boundary. There are many ways of doing that. For example, one could pick a base point on the surface where all cuts start and end. Then any handle could be turned into a single hole by two cuts, and two cuts for every other handle expand this hole. This would turn the surface into a  $4\gamma$ -gon with all its vertices at the base point, see Figure 3 for an illustration where a double torus is cut into an octagon on the left. To show that other cuts are possible, this figure also depicts another cut into a dodecagon.

A polygon forming such a closed surface  $S$  has pairs of identical edges and (groups of) identical vertices whose angles sum to  $2\pi$ . For any such surface polygon, there are similar polygons in the hyperbolic plane and we parametrize  $S$  over such a

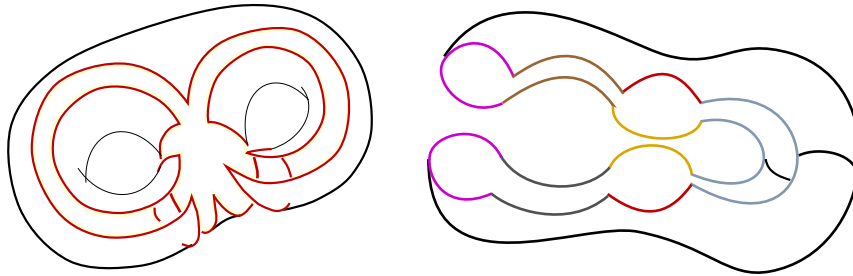


**Fig. 3** Cutting a double torus into an octagon and a dodecagon

polygon  $F$ . Here “similar” means that the edges of  $F$  with identical images on  $S$  are equally long and that the angles at the vertices with the same image on  $S$  sum to  $2\pi$ .

By two hyperbolic reflections, we can first map any edge of  $F$  onto its partner and secondly onto itself. These two reflections map  $F$  to an adjacent congruent polygon and, iterating this procedure, we obtain a partition of the hyperbolic plane into infinitely many congruent copies of  $F$ , see [20] and Figure 4 for an illustration, where the bold edge of the red tessellation on the right side is first reflected about line 1 and then about line 2.

The polygon  $F$  is called a **fundamental domain** and the hyperbolic isometries mapping  $F$  to any of the tiles above form a **Fuchsian group**  $G_F$ .

A smooth piecewise rational function  $\mathbf{s}$  mapping the hyperbolic plane  $\mathcal{H}^2$  to some closed surface  $S$  is called an **orbifold spline** if, for any member  $\varphi$  of  $G_F$ , we have

$$\mathbf{s} \circ \varphi = \mathbf{s}. \tag{2}$$

Hence an orbifold spline  $\mathbf{s}$  maps  $F$  and any isometric image of it onto the entire surface  $S$ ; in other words,  $\mathbf{s}$  wraps the hyperbolic plane  $\mathcal{H}^2$  infinitely often around  $S$  or “orbits” around  $S$ .

## 6 Projective Structures

From Sections 3 and 5, it follows that we can represent any orbifold spline consisting of rational triangular patches by a trivariate homogeneous piecewise polynomial spline, where

- the polynomial segments have Bézier forms with respect to tetrahedra
- that have the origin as a common vertex
- and represent a triangulation, i. e., a tessellation into triangles, of the hyperbolic plane  $\mathcal{H}^2$ .

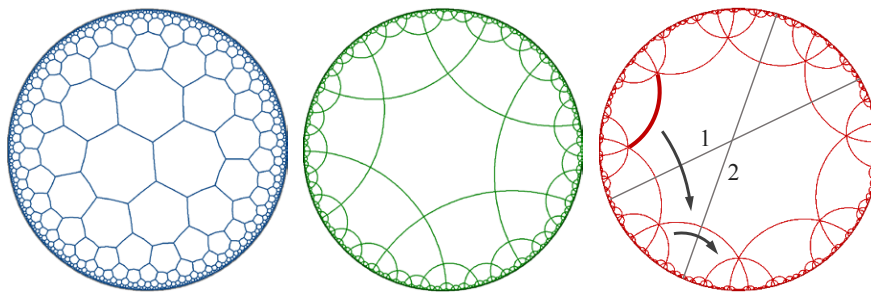


**Fig. 4** Tessellations of the hyperbolic plane into hexagons and octagons. The blue and green tessellations on the left side are hyperbolic images of each other.

The tetrahedra form a bunch of tetrahedra that span cones which, when intersected with the disk  $\mathcal{D}$  or the hyperboloid  $\mathcal{U}$ , give us a triangulation of  $\mathcal{H}^2$  in the Klein or hyperboloid model, respectively. Since the triangles of this triangulation are the parameter domains of the patches of an orbifold spline, which satisfies (2), the triangulation is mapped to itself by all members of the corresponding Fuchsian group.

If the homogeneous spline representation of any rational orbifold spline is in  $C^r$ , then the rational spline satisfies  $G^r$  conditions with projective, i. e., linear rational transition functions determined by the pairs of adjacent tetrahedra as discussed in Section 4. Note that, due to Remark 10, any linear image of two adjacent tetrahedra (or any projective image of two adjacent weighted triangles) defines the same  $G^r$  conditions.

**Definition 2** The set of transition functions above is called a **projective structure**.

*Remark 11* As an orbifold spline “wraps”  $\mathcal{H}^2$  infinitely often around the surface, it parametrizes any patch of the surface multiply over infinitely many triangles in  $\mathcal{H}^2$ . For each patch, we can pick one such triangle so as to get a connected domain for one covering of the surface. Thus, this domain is a fundamental domain  $F$  and the members of the Fuchsian group  $G_F$  map any triangle to all the other triangles that are the domains for the same patch. Hence,  $G_F$  induces an equivalence relation among the domain triangles such that any two triangles are equivalent if one of them can be mapped onto the other by some  $\varphi \in G_F$ .

*Remark 12* A projective structure is represented by the tetrahedral bunch above and can easily be changed into other projective structures for the same surface by moving the vertices of the tetrahedra (except for the origin) and splitting or collapsing tetrahedra freely as long as any change within a fundamental domain  $F$  is simultaneously transferred to all copies  $\varphi F$ ,  $\varphi \in G$ . In addition the interiors of the tetrahedra should stay disjoint to exclude self-overlapping spline surfaces.

*Remark 13* In the projective structure above, we can replace any tetrahedron  $\mathbf{abc}$  by a scaled version  $\mathbf{a}\alpha\mathbf{b}\beta\mathbf{c}\gamma$  of it and represent the spline with respect to the scaled tetrahedron, see Remarks 6 and 7. This does not change the surface, but its parametrization and transition functions. A canonical choice is to scale the vertices of a projective structure such that they lie on the hyperbolic sheet  $\mathcal{U}$ . This guarantees that the hyperbolic maps – in particular the ones in the Fuchsian group – map the set of all vertices into itself, see Remark 4 and below.

*Remark 14* The transition functions of tetrahedra  $A_1, \dots, A_n = A_0$  around common edges satisfy

$$\langle A_n A_{n-1}^{-1} \rangle \cdot \langle A_{n-1} A_{n-2}^{-1} \rangle \dots \langle A_1 A_0^{-1} \rangle = I,$$

which ensures that the derivatives up to order  $r$  of  $n$  patches around a common vertex end up being the same when we “pass them around” by the  $G^r$  conditions based on these transition functions.

*Remark 15* Restricting the homogeneous  $C^r$  representation of an orbifold spline to any plane not going through the origin gives a polynomial  $C^r$  spline over a planar triangulation. It is a bivariate spline where the periodicity, or orbifold condition (2), means that any spline patch equals infinitely many others that are all parametrized differently, as explained in Remark 7 (and Remark 6).

*Remark 16* There are several ways of getting a projective structure for an orbifold spline. All we need is the topology of the patch layout or network, i. e., the graph of the patch boundaries. For example, we can take any fundamental domain corresponding to cuts that open the patch network to a topologically planar bounded polygon and triangulate it arbitrarily but consistently with the patch layout and the Fuchsian group. Another possibility is to determine a triangulation of the hyperbolic plane for a given surface from the two conditions that (i) its hyperbolic angles around a vertex sum to  $2\pi$  and (ii) that edge lengths, which are used to compute the angles of a triangle, are equal for both triangles they belong to, see [3].

## 7 Quadrilateral orbifold splines with bi-projective structures

Our goal is to construct rational orbifold splines with quadrilateral tensor product patches based on triangular orbifold splines. While it is straightforward to use the tetrahedral Bézier form for rational triangular patches in homogeneous coordinates to build triangular orbifold splines, we cannot easily follow this approach for quadrilateral orbifold splines.

However, we can use pairs of adjacent triangular patches to determine quadrilateral patches with the same four boundary curves and  $G^r$  contact along those curves up to any derivative order. In this way it is possible to obtain quadrilateral orbifolds through triangular splines. In the following we present the details:

1. Given a quadrilateral patch layout for an orbifold spline, we split all quadrilaterals into pairs of triangles and compute a projective structure for it.
2. Over the projective structure, i. e., over the bunch of tetrahedra representing the projective structure, we build a piecewise homogeneous polynomial spline such that all pairs of its adjacent segments have  $C^r$  joints except for those over any two tetrahedral cones corresponding to a split quadrilateral. Between any two such segments, we require  $C^{2r}$  smoothness but only at the common edges of their cones. (Figure 6 shows a quadrilateral cone split into two triangular cones **abc** and **bcd** with common edges **bℝ** and **cℝ**.)
3. For any initially given quadrilateral, we compute a quadrilateral patch having  $G^r$  contact along the four boundary edges with the associated pair of triangular patches.

Step 3 is the essential part and we discuss it in detail: As in Section 4, let

$$r(\mathbf{A}\mathbf{u}) = \sum_{\mathbf{i} \in \Gamma_n^3} r_{\mathbf{i}} B_{\mathbf{i}}(\mathbf{u})$$

and

$$\mathfrak{s}(B\mathbf{u}) = \sum_{\mathbf{i} \in \Gamma_n^3} \mathfrak{s}_{\mathbf{i}} B_{\mathbf{i}}(\mathbf{u})$$

be two homogeneous polynomials given w.r.t. the triangles  $A = [\mathbf{abc}]$  and  $B = [\mathbf{bcd}]$ . We reparametrize them by the bi-linear map

$$\mathbf{x}(s, t) = \mathbf{a} B_{00}^{11}(s, t) + \mathbf{b} B_{10}^{11}(s, t) + \mathbf{c} B_{01}^{11}(s, t) + \mathbf{d} B_{11}^{11}(s, t), \quad (3)$$

where

$$B_{ij}^{nn}(s, t) = \binom{n}{i} s^i (1-s)^{n-i} \binom{n}{j} t^j (1-t)^{n-j}$$

are the tensor product Bernstein polynomials of bi-degree  $n$  and where  $s$  and  $t$  are the affine coordinates w.r.t. the affine system  $\mathbf{a}$ ,  $(\mathbf{b} - \mathbf{c})$ ,  $(\mathbf{c} - \mathbf{a})$ .

Thus, we get the bi-degree  $n$  tensor product polynomials

$$\mathfrak{r}(s, t) = \mathfrak{r}(\mathbf{x}(s, t)) = \sum \mathfrak{r}_{ij} B_{ij}^{nn}(s, t)$$

and

$$\mathfrak{s}(s, t) = \mathfrak{s}(\mathbf{x}(s, t)) = \sum \mathfrak{s}_{ij} B_{ij}^{nn}(s, t)$$

with  $C^{2r}$  contacts at  $\mathbf{b}$  and  $\mathbf{c}$  or their parameter values  $(1, 0)$  and  $(0, 1)$ , respectively. Consequently

$$\mathfrak{r}_{ij} = \mathfrak{s}_{ij}, \quad \text{for } i = j \pm k \quad \text{and } k \geq n - r.$$

The indices of the equal Bézier points  $\mathfrak{r}_{ij}$  and  $\mathfrak{s}_{ij}$  are marked by red dots in Figure 5 for  $n = 5$  and  $r = 1$ . The solid red dots show which Bézier points are equal if we required  $C^1$  joints at the vertices only and that then we could not ensure compatible corner twists for  $\mathfrak{r}$  and at  $(s, t) = (0, 1)$  and  $(1, 0)$ .

Hence, any tensor product patch

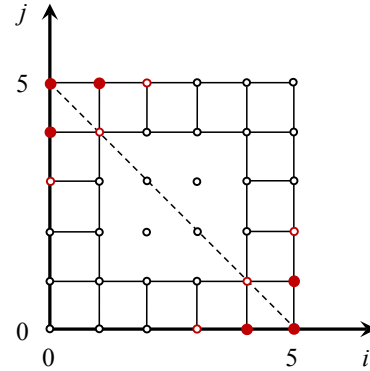


**Fig. 5** Indices of the equal Bézier points of two bi-quintic patches obtained by reparametrizing a pair of triangular patches with  $C^1$  (and  $C^2$ ) contact at the pair's common vertices with bold (and empty) red dots.



$$\mathbb{P}(s, t) = \sum_{i,j=0}^n \mathbb{P}_{ij} B_{ij}^{nn}(s, t)$$

with

$$\mathbb{P}_{ij} = \begin{cases} \mathfrak{r}_{ij}, & i \leq r \text{ or } j \leq r \\ \mathfrak{s}_{ij}, & i \geq n-r \text{ or } j \geq n-r \end{cases}$$

represents a rational polynomial of bi-degree  $n$  having  $G^r$  contact with the rational triangular patches  $\langle \mathfrak{r}(\mathbf{x}) \rangle$  and  $\langle \mathfrak{s}(\mathbf{x}) \rangle$  over the lines  $\langle \mathbf{ab} \rangle$  and  $\langle \mathbf{ac} \rangle$  or  $\langle \mathbf{cd} \rangle$  and  $\langle \mathbf{bd} \rangle$ , respectively. Note that the transition functions of these  $G^r$  contacts are bi-linear rational functions.

*Remark 17* The Bézier points  $\mathfrak{r}_{ij}$  can be obtained from the points  $\mathfrak{r}_i = \mathfrak{r}_{ijk}$  using polar forms. For instance, let

$$\mathfrak{r}[\mathbf{x}_1 \dots \mathbf{x}_n]$$

be the polar form of the trivariate homogeneous polynomial  $\mathfrak{r}(\mathbf{x})$ . Then we recall from, e.g., [17, Section 11.10] that  $\mathfrak{r}(s, t)$  has the tensor product polar form

$$\mathfrak{r}[s_1 \dots s_n | t_1 \dots t_n] = \frac{1}{n!} \sum_{\tau} \mathfrak{r}[\mathbf{x}(s_1, \tau_1) \dots \mathbf{x}(s_n, \tau_n)]$$

where the sum is taken over all permutations  $\tau = (\tau_1, \dots, \tau_n)$  of  $(t_1, \dots, t_n)$  and that

$$\begin{aligned} \mathfrak{r}_{ij} &= \mathfrak{r}[0 \overset{n-i}{.} 0 \ 1 \ . \ . \ . \ 1 | 0 \overset{n-j}{.} 0 \ 1 \ . \ . \ . \ 1] \\ &= \sum_{k=0}^j \beta_{ijk} \mathfrak{r}_{n+k-i-j, i-k, j-k, k} \end{aligned}$$

with

$$\beta_{ijk} = \frac{k!}{n!} \binom{i}{k} \binom{j}{k} \frac{(n-i)!(n-j)!}{(n+k-i-j)!}$$

and the points  $\mathfrak{r}_{\kappa\lambda\mu\nu}$  obtained after  $\nu$  steps of de Casteljau's algorithm to compute  $\mathfrak{r}(\mathbf{d})$  from the Bézier points

$$\mathfrak{r}_{ijk0} = \mathfrak{r}_i, \quad \mathbf{i} = \begin{bmatrix} i \\ j \\ k \end{bmatrix} \in \Gamma_n^3,$$

which means that

$$\mathfrak{r}_{\kappa\lambda\mu\nu} = \alpha \mathfrak{r}_{\kappa+1, \lambda, \mu, \nu-1} + \beta \mathfrak{r}_{\kappa, \lambda+1, \mu, \nu-1} + \gamma \mathfrak{r}_{\kappa, \lambda, \mu+1, \nu-1}$$

where

$$\mathbf{d} = \alpha \mathbf{a} + \beta \mathbf{b} + \gamma \mathbf{c}.$$

## 8 Quadrilateral orbifold splines with projective structures

The construction in Section 7 results in quadrilateral orbifold splines with rational bi-linear transition functions forming what we could call a **bi-projective structure** and, in general, there is no projective structure consisting of only projective transition functions for  $G^k$  quadrilateral orbifold splines that also lie in  $C^0$ , [16]. However, there are projective structures for such splines if we give up continuous transitions between the parametrizations of adjacent patches, and in this section we show how to build such  $C^{-1}/G^k$  splines. The construction is a special case of the one in Section 7, where we replace the bi-linear by linear reparametrizations.

For any quadrilateral  $\mathbf{abcd}$  in  $\mathbb{R}^3$  associated to a pair of triangular patches, we determine  $\alpha, \beta, \gamma, \delta$  such that  $\mathbf{a}\alpha, \mathbf{c}\gamma, \mathbf{b}\beta, \mathbf{d}\delta$  form a parallelogram. Such a parallelogram exists and is parallel to the intersections of each pair of opposite sides of the cone  $\mathbf{abdc}$  with apex  $\mathbf{o}$ , see Figure 6. Thus,

$$\mathbf{c}\gamma - \mathbf{a}\alpha = \mathbf{d}\delta - \mathbf{b}\beta$$

is a multiple of

$$(\mathbf{a} \times \mathbf{c}) \times (\mathbf{b} \times \mathbf{d}).$$

Since  $\mathbf{a}\alpha, \mathbf{c}\gamma, \mathbf{d}\delta, \mathbf{b}\beta$  is a parallelogram, it is an affine image of the unit square  $[0, 1]^2$  meaning that the bi-linear map  $\mathbf{x}(s, t)$  in (3) actually is a linear map. Consequently, if we reparametrize the pairs of triangular patches with these maps, we obtain quadrilateral patches in Section 7 that have  $G^r$  contacts with projective transition functions. However, in general, the scaling factors  $\alpha, \beta, \gamma, \delta$  can not be chosen consistently for adjacent quadrilaterals and inconsistent scaling factors mean that common boundary curves of adjacent patches are equal, but with different parametrizations. Their Bézier points are the same though, yet they have different weights, see Remark 6.

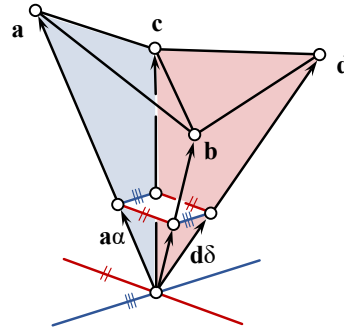


**Fig. 6** Intersecting a quadrilateral cone in a parallelogram.

## 9 Conclusions

So far, quadrilateral orbifold splines have been known only with low smoothness orders and certain restrictions on the patch layout. In this paper, we overcome these restrictions by a general construction that gives quadrilateral orbifold splines with an arbitrarily high smoothness order for any patch layout. This construction is based on rational triangular orbifold splines, which have a piecewise homogenous polynomial representation.

Piecewise polynomial triangular splines can be built using splitting techniques as, e. g., Powell-Sabin splits or by requiring supersmoothness at the vertices or by solving linear systems of  $C^k$  conditions, typically in addition to interpolation and fairness conditions. In general, we do not know the minimum degree needed for the latter solutions. The examples in [2, 3] show that the degree is considerably smaller than  $4k + 1$  for which it is known that supersmooth solutions always exist.

For the quadrilateral orbifold splines in this paper, we need triangular splines with supersmoothness at the vertices but, on the other hand, they can be non-smooth or even discontinuous along the edges corresponding to the diagonals that split the quadrilaterals into triangles. Thus the triangular splines that we propose to use for building quadrilateral orbifold splines might have similar low degrees than the ones in [2, 3]. We plan to discuss such practical issues and to present the outcomes of our implementations in a forthcoming paper.

**Acknowledgements** C. Beccari is a member of the INdAM Research group GNCS, which has partially supported this work.

## References

1. Alfeld, P., Neamtu, M., Schumaker, L. L.: Bernstein-Bézier polynomials on spheres and sphere-like surfaces. *Computer Aided Geometric Design* **13**, 333–349 (1996)
2. Beccari, C.V., Gonsor, D., Neamtu, M.: RAGS: Rational geometric splines for surfaces of arbitrary topology. *Computer Aided Geometric Design* **31**, 97–110 (2014)
3. Beccari, C.V., Neamtu, M.: On constructing RAGS via homogeneous splines. *Computer Aided Geometric Design* **43**, 109–122 (2016)
4. Boehm, W., Prautzsch, H.: *Geometric Concepts for Geometric Design*. A K Peters/CRC Press, New York (1994)
5. de Boor, C.: B-Form Basics. In Farin (ed.) *Geometric Modeling: Algorithms and New Trends*, pp. 131–148. Society for Industrial and Applied Mathematics, Philadelphia (1987)
6. Ferguson H., Rockwood A.: Multiperiodic functions for surface design. *Computer Aided Geometric Design* **10**, 315–328 (1993)
7. Gu, X., He, Y., Qin, H.: Manifold splines. *Graphical Models* **68**, 237–254 (2006)
8. Gu, X., He, Y., Jin, M., Luo, F., Qin, H., Yau, S.T.: Manifold splines with a single extraordinary point. *Computer Aided Design* **40**, 676–690 (2008)
9. Hilbert, D.: *Grundlagen der Geometrie*. Teubner (1903)
10. Hilbert, D., Cohn-Vossen, S.: *Anschauliche Geometrie*. 2nd ed. Springer (1996)
11. Kasten, H., Vogel, D.: *Grundlagen der ebenen Geometrie*. Springer Spektrum (2018)
12. Kowol, G.: *Projektive Geometrie und Cayley-Klein Geometrien der Ebene*. Birkhäuser (2009)

13. Peters J., Fan, J.: The projective linear transition map for constructing smooth surfaces. SMI 2010 – International Conference on Shape Modeling and Applications, Proceedings 2010, Article number 5521455, pp. 124–130 (2010)
14. Peters, J., Sarow, M.: Polynomial spline surfaces with rational linear transitions *Computers & Graphics*, Volume 51, 43-51 (2015)
15. Prautzsch, H: Freeform splines. *Computer Aided Geometric Design* **14**, 201–206 (1997)
16. Prautzsch, H: Spline Orbifold Constructions. Talk at the SIAM Conference on Industrial and Applied Geometry, 10-12 July 2017, Pittsburgh
17. Prautzsch, H., Boehm, W., Paluszny, M.: *Bézier and B-Spline Techniques*. Springer-Verlag Berlin Heidelberg (2002)
18. Prautzsch, H., Reif, U.: Degree estimates for  $C^k$ -piecewise polynomial subdivision surfaces. *Advances in Computational Mathematics* **10**, 209–217 (1999)
19. Pottmann, H., Wallner, J.: Spline orbifolds. In: Le Méhauté, A., Rabut, C., Schumaker, L. (eds.), *Curves and Surfaces with Applications in CAGD*, pp. 445–464. Vanderbilt University Press, Nashville, TN (1997)
20. Ratcliffe, J.G.: *Foundations of Hyperbolic Manifolds*, 2nd ed. *Grad. Texts Math.*, vol. 149. Springer-Verlag, New York (2007)
21. Reif, U.: A degree estimate for subdivision surfaces of higher regularity. *Proceedings of the AMS* **124**, Number 7, 2167–2174 (1996)
22. Reif, U.: TURBS – Topologically Unrestricted Rational B-Splines. *Constructive Approximation* **14**, 57–77 (1998)
23. Sarov, M., Peters J: Refinable polycube G-splines. *Computers & Graphics* **58**, 92–101 (2016)
24. Wallner, J.: *Geometric contributions to surface modeling*. PhD thesis. Vienna University of Technology (1996)